Available online at www.sciencedirect.com

ScienceDirect

journal homepage: www.elsevier.com/locate/he

Co/CuO–NiO–Al_2O_3 catalyst for hydrogen generation from hydrolysis of $NaBH_4$

Neslihan Erat [a], Gamze Bozkurt [b], Abdulkadir Özer [a,*]

[a] Chemical Engineering Department, Atatürk University, Erzurum, 25240, Turkey
[b] Project Coordination Implementation and Research Center, Erzurum Technical University, Erzurum, 25050, Turkey

HIGHLIGHTS

- Co/CuO–NiO–Al_2O_3 catalyst activity was investigated in $NaBH_4$ hydrolysis for the first time.
- Hydrogen generation from $NaBH_4$ were carried out in a system designed by our group.
- Maximum hydrogen generation rate was measured to be 2067.2 ml min^{-1} g_{cat}^{-1} at 25 °C.
- Promising catalyst activity was achieved with low activation energy of 31.59 kJ mol^{-1}.

GRAPHICAL ABSTRACT

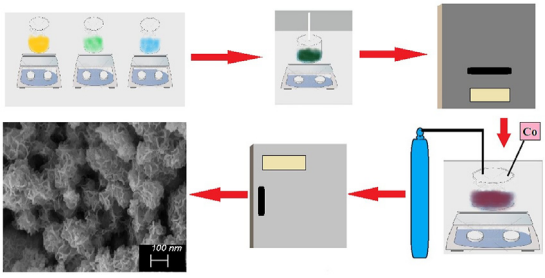

ARTICLE INFO

Article history:
Received 20 March 2022
Received in revised form
16 May 2022
Accepted 20 May 2022
Available online 9 June 2022

Keywords:
Trimetallic oxide support
Co/CuO–NiO–Al_2O_3 catalyst
Sodium borohydride
Hydrolysis
Hydrogen generation

ABSTRACT

This paper presents hydrogen generation measurements from the hydrolysis of $NaBH_4$ aqueous solutions catalyzed by Co doping on single, bimetallic and trimetallic oxide supports (Co/CuO, Co/NiO, Co/Al_2O_3, Co/NiO–Al_2O_3, Co/CuO–Al_2O_3, and Co/CuO–NiO–Al_2O_3). Support materials are synthesized by the co-precipitation method. Then, Co is doped into support materials by the impregnation method. It is found that Co/CuO–NiO–Al_2O_3 catalyst exhibited high reaction activity with a maximum hydrogen generation rate (HGR) of 2067.2 ml min^{-1} g_{cat}^{-1} at 25 °C. The effect of temperature of the solution, Co amount, and recyclability of the catalyst on hydrogen generation with Co/CuO–NiO–Al_2O_3 catalyst is investigated in detail. In addition, the highest HGR for Co/CuO–NiO–Al_2O_3 catalyst is obtained at 55 °C as 6460.0 ml min^{-1} g_{cat}^{-1}. The activation energy is calculated to be 31.59 kJ mol^{-1} using Co/CuO–NiO–Al_2O_3 catalyst. Co/CuO–NiO–Al_2O_3 catalyst exhibits zero-order reaction kinetics concerning $NaBH_4$ concentration. In addition, the Co/CuO–NiO–Al_2O_3 catalyst provided high reusability after 5 cycles.

© 2022 Hydrogen Energy Publications LLC. Published by Elsevier Ltd. All rights reserved.

* Corresponding author.
E-mail addresses: kadirozer@atauni.edu.tr, abdulkadirozer04@gmail.com (A. Özer).
https://doi.org/10.1016/j.ijhydene.2022.05.178
0360-3199/© 2022 Hydrogen Energy Publications LLC. Published by Elsevier Ltd. All rights reserved.

Introduction

Due to the increasing population and energy-consuming lifestyle, the energy production technologies that are being used have started to cause environmental problems [1–4]. This situation shows that environmentally friendly processes should be given a chance. Due to its high energy density, zero emissions, and abundant resources, hydrogen is the most promising candidate to replace the non-renewable fuel sources used today [5–10]. The most commonly used hydrides for hydrogen production are $NaBH_4$, LiH, KBH_4, $NaAlH_4$, $LiBH_4$, $N_2H_4BH_3$, and NH_3BH_3 [11–14]. Among these practical borohydrides, sodium borohydride ($NaBH_4$) has the advantage in terms of its high hydrogen density, non-flammability, non-toxicity, being able to be used in fuel cells, and being able to become a solution with water and alcohols [15,16].

$$NaBH_4 + 2H_2O \rightarrow NaBO_2 + 4H_2 \quad (1)$$

In the reaction given in Eq. (1), the catalyst is very important in increasing the reaction rate and controlling the reaction. Therefore, the reaction rate can be improved by using suitable catalysts [17–19]. Generally, noble metal catalysts such as Ru [20], Pd [21], Pt [22,23], and Rh [24] predominate, due to their superior catalytic properties. However, their high prices and limited supplies reduce their use as catalysts. Therefore, there is increasing interest in the development of non-noble metal catalysts to replace these noble metals, which are inexpensive, readily available, and have efficiency comparable to noble metals [25].

Transition metal catalysts such as Co, Ni, Cu, and Fe are used as alternatives to noble metals in the hydrolysis of $NaBH_4$. Cobalt is one of the most widely used active metals and shows better catalytic activity than other transition metal catalysts [26–28]. Co catalyst synthesized using $CoCl_2$ as a precursor has the highest catalytic activity compared to Co synthesized using $Co(NO_3)_2$, $Co(CH_3COO)_2$, and $CoSO_4$ [29–31].

Mixed metal oxides can play a remarkable role in many areas of chemistry and physics. Mixed metal oxides are widely used as both catalyst and catalyst supports. Mixed metal oxides are substances that, when added to the structure, increase the activity, selectivity, and stability of the active ingredient to achieve the desired activity. Although many methods have been used to prepare mixed metal oxides, co-precipitation (wet precipitation) is the most widely used method [32,33].

The support materials act as a carrier by providing a high surface area for the active component in the catalyst. Moreover, it improves the homogeneous distribution and the high catalytic performance of the catalyst. The use of support material also facilitates the physical separation of the catalyst from the reaction medium. It increases the active sites on the surface of the material and prevents agglomeration or aggregation. The interaction between catalytic metals and support materials is very important in increasing catalytic activity and durability. The long-term stability of the selected support in the reaction environment and its physical strength are important criteria. In addition, the chemical compatibility of the support and the catalyst particles, economical, and ease of production are the features sought in selecting the support [34,35]. Al_2O_3 [36], SiO_2 [37], TiO_2 [38], attapulgite clay [39], graphene oxide [40], Dowex 50WX8 resin [41], Ni foam [42], aluminum phosphate [43], Amberlite IRC-748 [11], and zeolite [44] are widely used in H_2 production as support materials. In addition, in our previous studies, Co_3O_4 was used as a support for noble metals such as Ni, Co, Ru, Pt, and Pd nanoparticles [23,45].

Although there are many studies in the literature on the use of a single support-containing catalyst for catalytic hydrogen generation from $NaBH_4$, no study has been found on catalysts containing double and triple metal oxide support. For this purpose, in this study, Co/Al_2O_3, Co/CuO, Co/NiO as single metal oxide support-containing catalyst, $Co/CuO–Al_2O_3$, $Co/NiO–Al_2O_3$ as bimetallic oxide support-containing catalyst, and $Co/CuO–NiO–Al_2O_3$ as trimetallic oxide support-containing catalyst was synthesized by co-precipitation and chemical impregnation methods. The activities of the synthesized catalysts were measured in an H_2 production system previously designed by our group. Experiment results show that the $Co/CuO–NiO–Al_2O_3$ catalyst exhibits high catalytic activity towards the hydrolysis reaction. The $Co/CuO–NiO–Al_2O_3$ catalyst in H_2 production was used for the first time in this study. $Co/CuO–NiO–Al_2O_3$ catalyst was characterized by XRD, SEM, TEM, and XPS analysis. The effect of temperature of the solution, catalyst amount, and recyclability of the catalyst on the catalytic activity for $NaBH_4$ hydrolysis was investigated. In addition, the activation energy and reaction order of the $Co/CuO–NiO–Al_2O_3$ catalyst were determined. $Co/CuO–NiO–Al_2O_3$ catalyst has been brought to the literature.

Experimental section

Materials

Sodium borohydride ($NaBH_4$, 98%), cobalt chloride hexahydrate ($CoCI_2.6H_2O$, 99%), aluminum chloride hexahydrate ($AlCI_3.6H_2O$, 99%), nickel chloride hexahydrate ($NiCI_2.6H_2O$, 99%), copper chloride dihydrate ($CuCI_2.2H_2O$, 99%), sodium hydroxide (NaOH), and ethanol (C_2H_5OH) were purchased from Merck. Deionized water was used in all experiments.

Synthesis of support material

A co-precipitation method was used to synthesize the trimetallic oxide support ($CuO–NiO–Al_2O_3$). 0.1 M $AlCI_3.6H_2O$, 0.1 M $NiCI_2.6H_2O$, and 0.1 M $CuCl_2.2H_2O$ were dissolved in 50 ml of deionized water in different beakers and stirred at 60 °C for 30 min on a magnetic stirrer. Then the solutions were combined and the metal hydroxides were precipitated by adding 1 M NaOH dropwise. The resulting mixture was stirred at 60 °C for 5 h. The precipitates were filtered and washed many times with deionized water and ethanol then dried in a drying oven at 100 °C for 4 h. Finally, the dried samples were annealed at 500 °C for 3 h under an air atmosphere. Single metal oxide (CuO, NiO, Al_2O_3) and bimetallic oxide ($NiO–Al_2O_3$, $CuO–Al_2O_3$) support materials were synthesized by a similar method.

Catalyst preparation

A certain amount of $CoCI_2.6H_2O$ was dissolved in 25 ml ethanol in a flask, then the required support material amount was added and the metal was adsorbed on the support material at room temperature for 24 h. The ethanol was removed from the medium at 50 °C and then 25 ml of deionized water was added to the Co-doped CuO–NiO–Al_2O_3 support material. The molar ratio of $NaBH_4$ reducing solution to the metal was taken as 3, and it was added dropwise under vigorous stirring. The reduction step was carried out in an ice-water bath to reduce the severity of the reaction. The black precipitate was filtered and rinsed several times with deionized water to remove all impurities. The obtained black powder was then dried at 100 °C for 4 h in an Ar atmosphere. The synthesized Co/CuO–NiO–Al_2O_3 catalyst was maintained in a closed vessel to use in the $NaBH_4$. The metal loading of Co on the support was taken as 5-10-15-20% by weight. Co/CuO, Co/NiO, Co/Al_2O_3, Co/NiO–Al_2O_3, and Co/CuO–Al_2O_3 catalysts were synthesized by a similar method.

Material characterization

The crystal structures of prepared samples were determined by X-ray diffraction (XRD) (PANalytical Empyrean). The surface morphology and elemental analysis of the synthesized catalyst and support were observed by scanning electron microscopy (SEM) (Zeiss Sigma 300) equipped with an energy dispersive X-ray detector (EDAX). The microstructures of the synthesized catalyst and support were examined by transmission electron microscopy (TEM, Hitachi HighTech HT7700). The chemical state of Co, Ni, Cu, and Al metals in the Co/CuO–NiO–Al_2O_3 catalyst is characterized by X-ray photoelectron spectroscopy (XPS) (Specs-Flex). Co content in the CuO–NiO–Al_2O_3 catalyst was confirmed by an ICP/MS (Agilent 7800) analyzer.

Hydrogen generation testing

The hydrogen generation system was designed by our group [23,45]. The schematic diagram of the system is shown in Fig. 1. To measure the HGRs, the Co/CuO–NiO–Al_2O_3 catalyst was placed in fiberglass and mounted in the tubular glass reactor. The prepared $NaBH_4$ and NaOH solutions are transferred to the reactor. The mass transfer between the catalytic surface and the solution was increased by continuously circulating the $NaBH_4$ and NaOH solution on the catalyst surface by a peristaltic pump until the reaction was completed. The hydrogen gas produced was dried to remove water vapor before being sent to the H_2 flow meter. The medium temperature was set to the desired temperature with the help of a PID controller. The cooling process was done by the main water system. The generated H_2 volume data were transferred to the computer via software. The HGR was found from the slope of the graph of hydrogen volume generated versus time in the linear region. The experiments were carried out three times, and the data's average was used.

Results and discussion

Characterization of catalyst

Fig. 2a illustrates XRD patterns for CuO–NiO–Al_2O_3 support material, Co/CuO–NiO–Al_2O_3 catalyst, and the 5th cycle experiment after the hydrolysis. Fig. 2b demonstrates CuO, NiO, Al_2O_3 metallic oxides and Co/CuO, Co/NiO, Co/Al_2O_3, Co/NiO–Al_2O_3, Co/CuO–Al_2O_3 catalysts. As is shown in Fig. 2a the sharp and strong peaks observed at 35°, 38°, 48.5°, and 61.7° positions with (002), (111), (−202), and (−113) indicate that the sample is having high crystalline quality CuO (tenorite). In addition, the peaks at 2θ of 43.1°, 62.6°, and 74.9° have been identified as peaks of cubic NiO crystallites with various diffraction planes (200), (220), and (311). Characteristic peaks of Al_2O_3 corresponding to 2θ values of 35°, 38°, and 43.1° may overlap CuO and NiO, respectively. According to the XRD patterns taken for the catalyst and 5th cycle experiment after the hydrolysis experiments around 50.3° peaks belong to Co. Also, the peak at 62.7 can be attributed to the peak of the (220) plane of CoO. In addition, the peak around 18° for the 5th cycle experiment after hydrolysis indicates the by-product $Na_2BO_2(OH)$ formed during the reaction [46]. It is seen that Co/

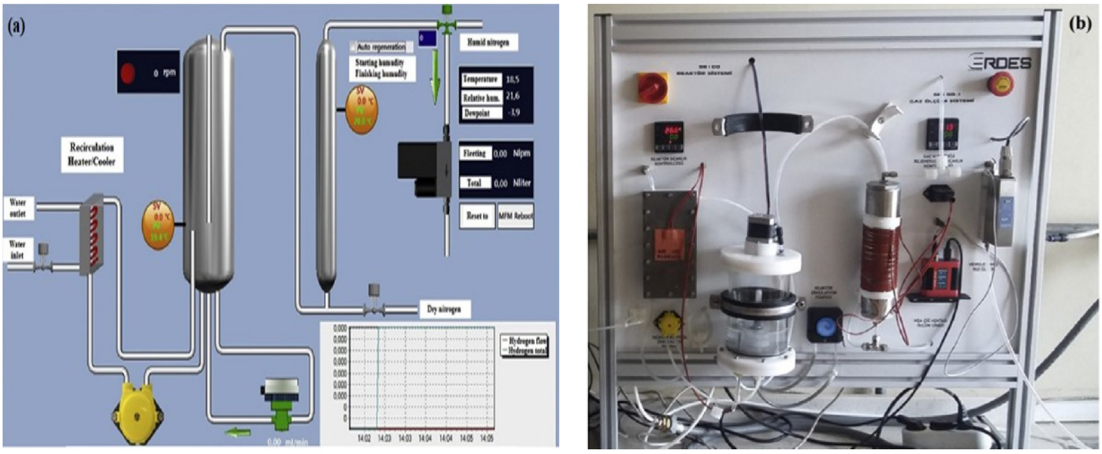

Fig. 1 – Hydrogen generation system (a) schematic diagram (b) photo of the designed system by our group [23,45].

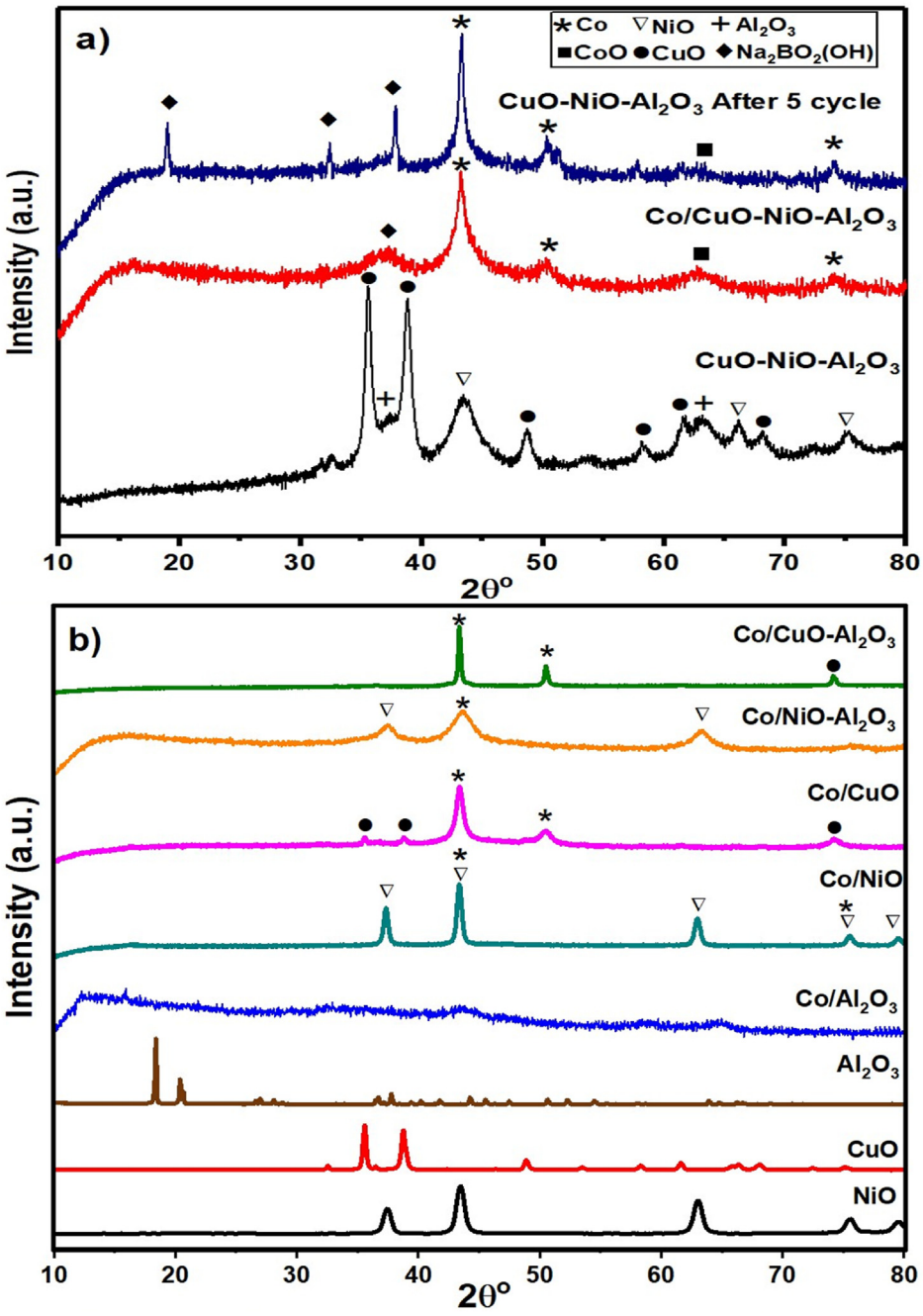

Fig. 2 – XRD patterns for a) CuO–NiO–Al_2O_3 support material, Co/CuO–NiO–Al_2O_3 catalyst, and Co/CuO–NiO–Al_2O_3 catalyst after five cycle and b) CuO, NiO, Al_2O_3 metallic oxides and Co/CuO, Co/NiO, Co/Al_2O_3, Co/NiO–Al_2O_3, Co/CuO–Al_2O_3 catalysts.

Al_2O_3 catalyst has amorphous structure and Co peak is dominant in Co/CuO, Co/NiO, Co/NiO–Al_2O_3, and Co/CuO–Al_2O_3 catalysts (Fig. 2b).

The SEM images of the CuO–NiO–Al_2O_3 support material and Co/CuO–NiO–Al_2O_3 catalyst are given in Fig. 3a–d. As can be seen in Fig. 3a, the agglomerated nanoparticles are formed in the support material, which could be due to the sintering at a high calcination temperature (500 °C). However, it has been observed that the catalyst has a homogeneous spongy structure (Fig. 3c). According to EDS spectrums (Fig. 3b and d) Cu, Ni, Al, and O elements are detected for the support material. In addition, Co peaks are observed for Co/CuO–NiO–Al_2O_3 catalyst.

TEM micrograph analysis is performed to determine clear detailed morphology and average nanoparticle shape and size. TEM micrograph analysis results for CuO–NiO–Al_2O_3 support material and Co/CuO–NiO–Al_2O_3 catalyst are given in Fig. 4a and b. According to the TEM image in Fig. 4a, non-homogeneous distribution is seen on the support material. In the TEM image of the Co/CuO–NiO–Al_2O_3 catalyst, it was determined that the Co particles overlapped and the particle boundaries could not be seen (Fig. 4b).

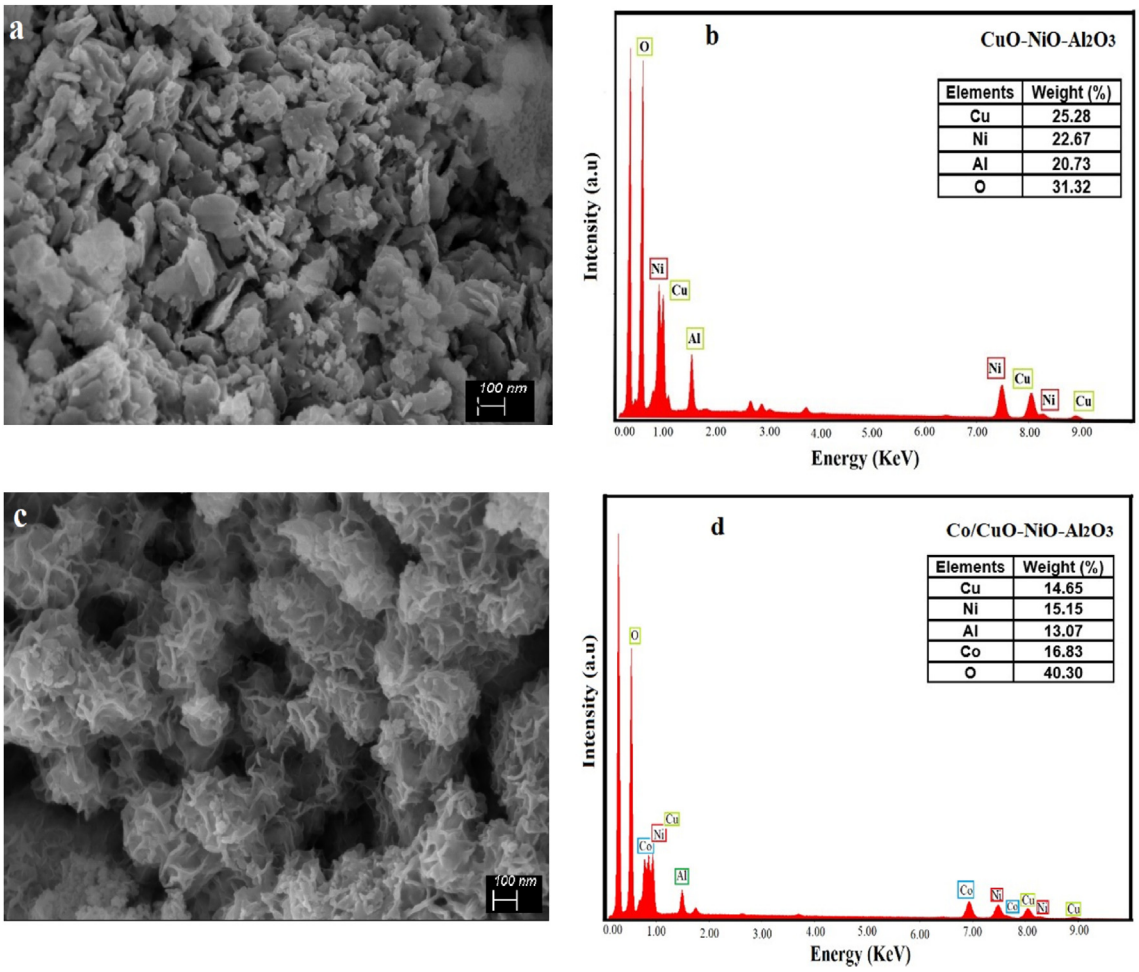

Fig. 3 – SEM images and EDS results of (a–b) CuO–NiO–Al_2O_3 support material, (c–d) Co/CuO–NiO–Al_2O_3 catalyst.

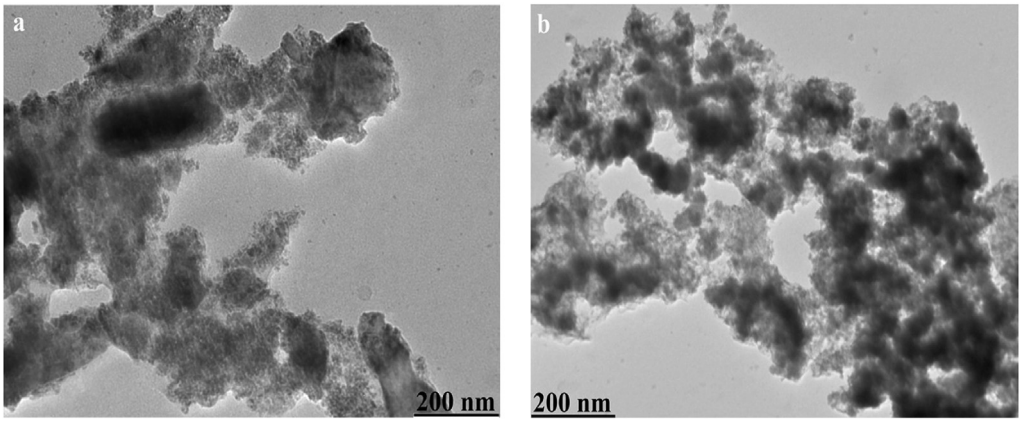

Fig. 4 – TEM images (a) CuO–NiO–Al_2O_3 support material, (b) Co/CuO–NiO–Al_2O_3 catalyst.

The valence states of different elements of Co/CuO–NiO–Al_2O_3 catalyst were further analyzed by X-ray photoelectron spectroscopy (XPS). The full survey spectrum (Fig. 5a) confirmed the existence of Cu, Co, Ni, Al, and O elements. As shown in Fig. 5b, the binding energies of Co $2p_{1/2}$ and Co $2p_{3/2}$ respectively at 795.9 and 779.2 binding energy is assigned to cobalt in metallic Co, which agree well with the XRD results, as seen in Fig. 2. The peaks located at 783.9 and 802.4 eV are typical satellite peaks. The satellite peak is usually caused by the "shakeup" process when excess electrons are excited to higher energy states. The binding energy at 797.8 and 780.1 eV corresponded to the Co $2p_{1/2}$ and Co $2p_{3/2}$, respectively, which confirms the existence of Co^{2+} [47]. The CoO seen in the XRD peaks is the result of oxidation on the metallic cobalt surface during catalyst preparation and storage [48]. Ni 2p XPS spectrum can also be divided into two-part

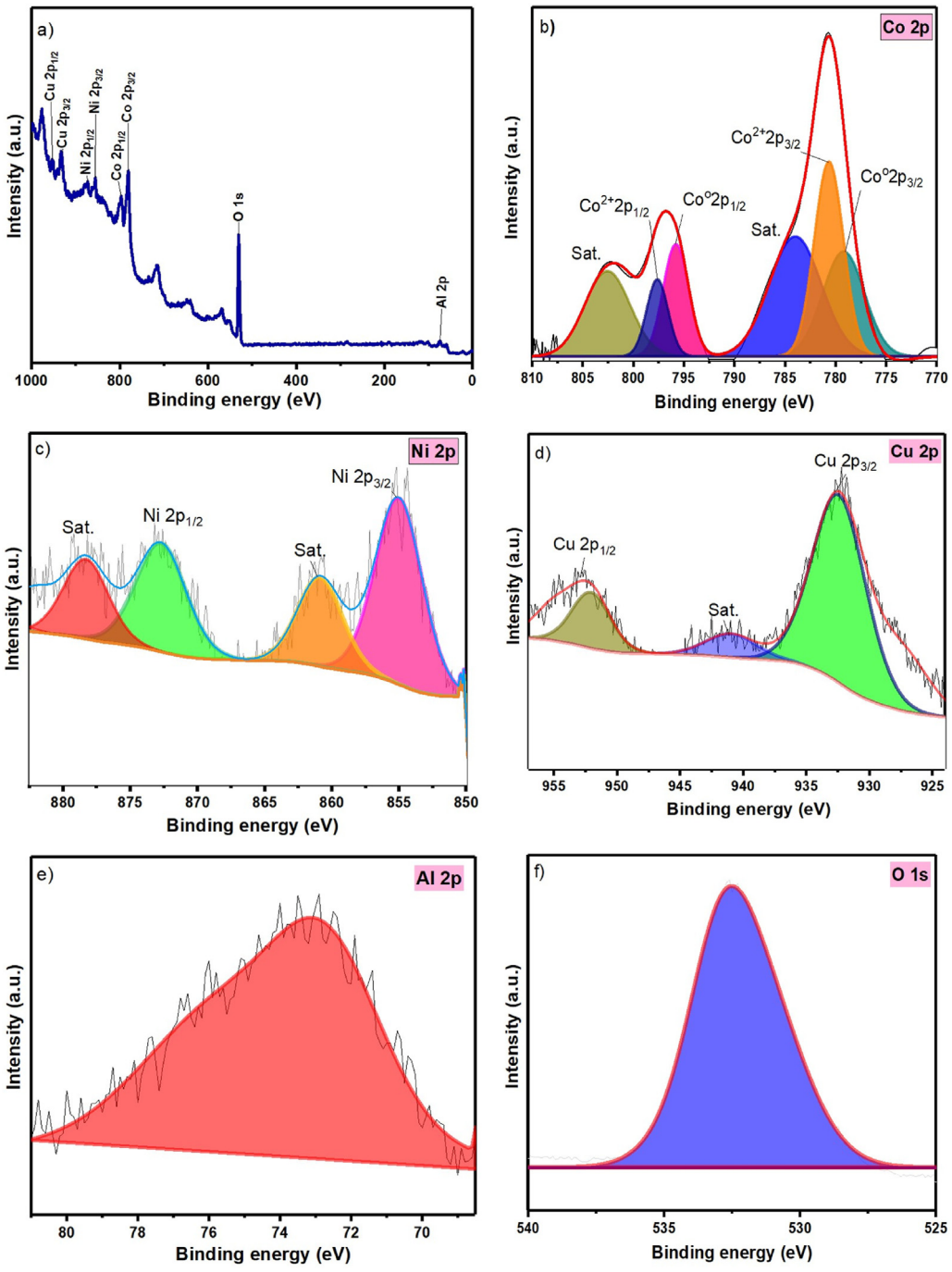

Fig. 5 – XPS spectrums for Co/CuO–NiO–Al_2O_3 catalyst (a) general spectrum (b) Co 2p (c) Ni 2p (d) Cu 2p (e) Al 2p (f) O 1s electron regions.

composed of Ni $2p_{1/2}$ and Ni $2p_{3/2}$, as shown in Fig. 5c. The binding energies of Ni 2p are 855.3 and 872.9 eV, which can be attributed to Ni $2p_{3/2}$ and Ni $2p_{1/2}$ peaks, respectively, which confirms the existence of Ni^{2+}. In addition, two peaks at 878.4 and 860.9 eV are assigned to shake-up satellite peaks of Ni $2p_{1/2}$ and Ni $2p_{3/2}$ species, respectively [49]. It can be seen from Fig. 5d that the Cu 2p energy level was composed of main characteristic doublet peaks corresponding to Cu $2p_{1/2}$ and Cu $2p_{3/2}$ at 952.2 and 932.6 eV, respectively, which confirms the existence of Cu^{2+}. A broad peak located at 941.2 eV can be the typical satellite peak of Cu $2p_{3/2}$, which shake-up satellite structure at about 11 eV binding energy higher than that of the main peak. They are known to be characteristics of the CuO phase and are in good agreement with the values reported in the literature [50]. The binding energy of 73.2 eV is well fitted in the Al 2p XPS spectrum as depicted in Fig. 5e, corresponding to the oxidation state of Al_2O_3. The binding energy of O 1s obtained at 532.6 eV corresponds to O^{2-} ions in the Co/CuO–NiO–Al_2O_3 catalyst (Fig. 5f). Co content in the catalyst was determined by ICP-MS analysis. The metal loading

percentage is found as 16.267 for Co. The Co loading value was found to be close to the target nominal value, 20 wt%.

The catalytic activity of catalysts with different supports

The catalysts Co-doped on single, bimetallic, and trimetallic oxide (Co/CuO, Co/NiO, Co/Al_2O_3, Co/NiO–Al_2O_3, Co/CuO–Al_2O_3, and Co/CuO–NiO–Al_2O_3) were used to hydrolysis of $NaBH_4$. To compare the catalysts, the activity tests were investigated individually using 50 mg catalyst, 5 wt% $NaBH_4$, 5 wt% NaOH solutions at 25 °C. The CuO–NiO–Al_2O_3 support without cobalt doping was also used as a catalyst for hydrogen generation under the same conditions. In the experiments, it was observed that hydrogen production did not occur. It indicates that CuO–NiO–Al_2O_3 support without cobalt has no catalytic activity. Fig. 6a shows the comparative curves of hydrogen production volumes for six catalysts and Fig. 6b shows the HGR values. As can be seen from Fig. 6a and b, when the activities of single-metallic supported catalysts are compared, Co/Al_2O_3 catalyst showed the lowest activity and

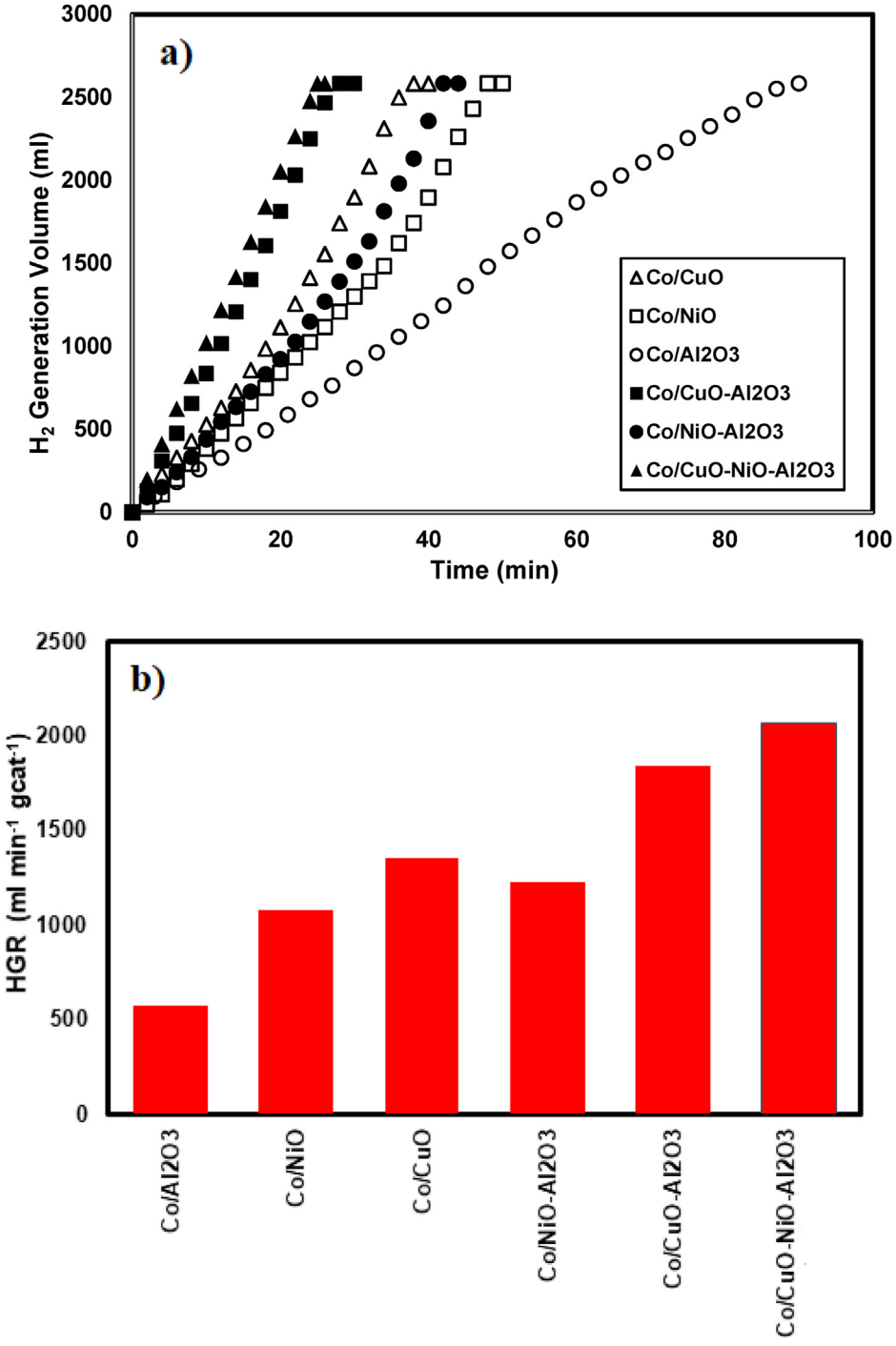

Fig. 6 – (a) Comparison of catalytic activity, (b) HGRs of Co-based catalysts with different support materials.

Co/CuO catalyst showed the highest activity for the $NaBH_4$ hydrolysis reaction. On the other hand, in bimetallic supported catalysts Co/CuO–Al_2O_3 catalyst showed higher activity than Co/NiO–Al_2O_3 catalyst. The experimental results showed that Co/CuO–NiO–Al_2O_3 was indeed the best catalyst compared to other synthesized catalysts, with an HGR value of 2067.2 ml min^{-1} g_{cat}^{-1} at 25 °C. Although the CuO–NiO–Al_2O_3 support without cobalt did not show catalytic activity for hydrogen production, it was determined that the catalytic activities of the catalysts containing CuO in the support material were higher than the catalysts containing NiO and Al_2O_3 among the Co-doped and reduced catalysts. We can think that as a result of the formation of new active sites, especially in CuO, in the support material during the hydrolysis reaction, the catalytic activity of Co/CuO–NiO–Al_2O_3 increases compared to other catalysts.

Catalysts using hybrid support materials are more effective than single-supported catalysts due to the increased active site [51]. Therefore, The Co/CuO–NiO–Al_2O_3 catalyst was chosen for further studies of the hydrogen generation reaction. There are many different catalysts used for H_2 production in the literature; however, the H_2 production performance of the Co/CuO–NiO–Al_2O_3 catalyst was described for the first time in this study.

Effect of cobalt amount on catalytic activity

The effect of different Co amounts (5, 10, 15, and 20 wt%) on the catalytic activity of the Co/CuO–NiO–Al_2O_3 catalyst was investigated for hydrolysis reaction, and the results are given in Fig. 7. Activity tests were performed using 50 mg catalyst, 5% $NaBH_4$, and 5% NaOH solutions at 25 °C. It can be seen that the HGR gradually increases with increasing the Co amount from 5 to 20 wt%, which can be ascribed to the improved cobalt content in Co/CuO–NiO–Al_2O_3 catalysts. The maximum HGRs for Co/CuO–NiO–Al_2O_3 catalyst containing 5, 10, 15, and 20 wt% Co amounts were found to be 202.8, 522.1, 1174.5, and 2067.2 ml min^{-1} g_{cat}^{-1}, respectively. As seen in the experimental results, the highest HGR was obtained for the 20 wt% Co-doped Co/CuO–NiO–Al_2O_3 catalyst. For this reason, 20 wt% Co-doped Co/CuO–NiO–Al_2O_3 catalyst was chosen for further studies of the hydrogen generation reaction.

Effect of temperature on catalytic activity

To determine the effect of temperature on the hydrolysis reaction by 20 wt% Co-doped Co/CuO–NiO–Al_2O_3 catalyst and to calculate the activation energy, the experiments were carried out at four different temperatures (25, 35, 45, and 55 °C) with 5 wt% $NaBH_4$, 5 wt% NaOH and 50 mg catalyst amount. Fig. 8 shows the H_2 generation volume versus the time graph for Co/CuO–NiO–Al_2O_3 catalyst at different temperatures. It is determined that the HGR is remarkably increased with the increase in the reaction temperature. The HGRs for Co/CuO–NiO–Al_2O_3 catalyst at 25, 35, 45, and 55 °C were found to be 2067, 2871, 4307, and 6460 ml min^{-1} g_{cat}^{-1}, respectively. The activation energy (Ea) was determined by using the Arrhenius equation and was calculated as 31.59 kJ mol^{-1} from the ln k versus 1/T graph for Co/CuO–NiO–Al_2O_3 catalyst, (Fig. 9). In Table 1, the HGR and Ea values of the previously reported Co-based catalysts and Co/CuO–NiO–Al_2O_3 catalyst for the hydrolysis of $NaBH_4$ are given. The Ea value in the Co/CuO–NiO–Al_2O_3 catalyst appears to be lower than the Ea value of the reported catalysts. In addition, the Co/CuO–NiO–Al_2O_3 catalyst showed hopeful activity with high HGR than most of the Co-based catalysts. Fig. 10 shows the changes in $NaBH_4$ concentration versus time at different

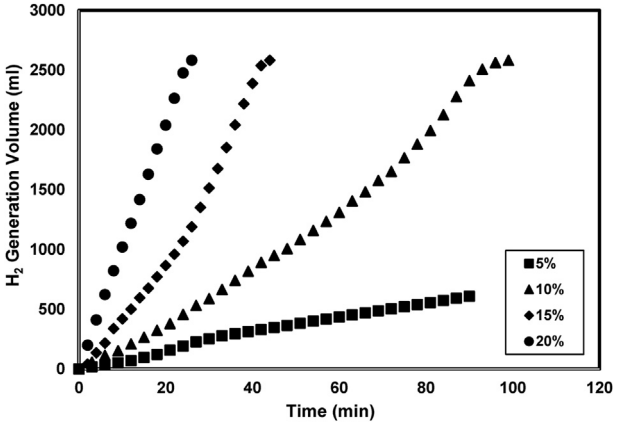

Fig. 7 – Effect of Co amount on catalytic activity of Co/CuO–NiO–Al_2O_3 catalyst.

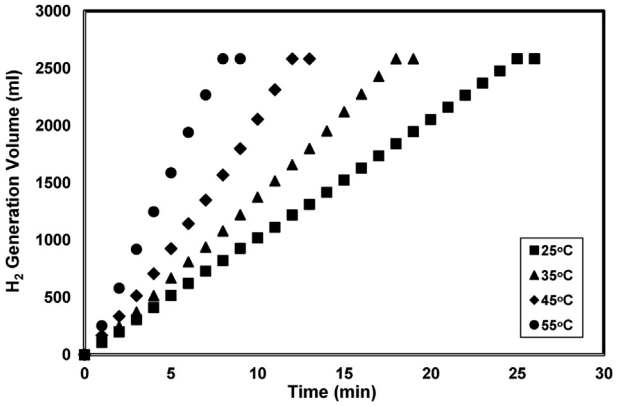

Fig. 8 – Effect of temperature on Co/CuO–NiO–Al_2O_3 catalyst.

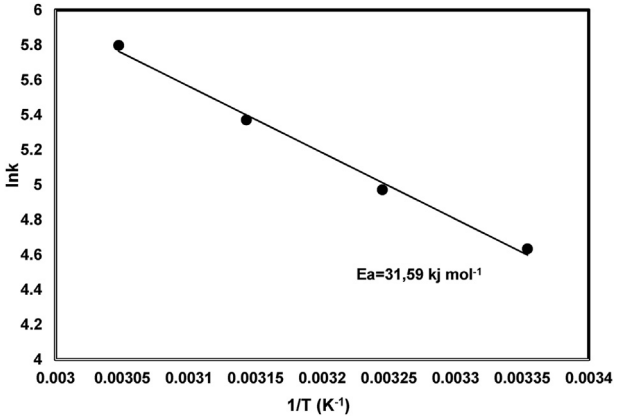

Fig. 9 – The corresponding Arrhenius plot of ln k vs 1/T.

Table 1 – Comparison of hydrogen generation performance of various cobalt-based catalysts.

Catalyst	Conditions	HGR (ml min^{-1} g^{-1})	Ea (kJ mol^{-1})	Ref.
Co/C_2N	10% $NaBH_4$ and 5% NaOH, 30 °C	8903	66.17	[52]
CoB/TiO_2	1% $NaBH_4$ and 3.75% NaOH, 30 °C	12,503	51	[17]
Ru/Ni Foam	5% $NaBH_4$ and 2% NaOH, 30 °C	23,030	–	[53]
CoMoNi–B/ZIF-67	3.7% $NaBH_4$ and 20% NaOH, 25 °C	6277	35.01	[54]
Co/IRC748	15% $NaBH_4$ and 5% NaOH, 30 °C	211	46.9	[11]
Co–Zn/Ni	10% $NaBH_4$ and 5% NaOH, 25 °C	455	50.2	[55]
MMT-H_3PO_4–Co–B	5% $NaBH_4$ and 1% NaOH, 30 °C	1869	49.5	[56]
Co–Ni/MWAC	5% $NaBH_4$ and 5% NaOH, 30 °C	111	53.06	[57]
CoB/Na-Bentonit	5% $NaBH_4$ and 10% NaOH, 50 °C	1601.45	56.61	[58]
Fe–Co–B/Ni Foam	15% $NaBH_4$ and 5% NaOH, 30 °C	221	27	[59]
Co–B/Ni Foam	25% $NaBH_4$ and 3% NaOH, 20 °C	700	45	[60]
Co/SiO_2	5% $NaBH_4$ and 5% NaOH, 40 °C	2513	–	[61]
Co–Ni–Fe–P	10% $NaBH_4$ and 1% NaOH, 30 °C	1128	54.26	[62]
Cu–Co–P/γ-Al_2O_3	5% $NaBH_4$ and 5% NaOH, 25 °C	1115	47.8	[63]
Ni/SiO_2	5% $NaBH_4$ and 5% NaOH, 40 °C	307	59	[64]
Co@ZIF-8	3% $NaBH_4$, 30 °C	7230	–	[65]
$ZrOSO_4/C$	3% $NaBH_4$, 25 °C	1666	–	[66]
CuO@C	0.05 M $NaBH_4$, 25 °C	7240	–	[67]
Co-CeO_x/NCNS	200 mM $NaBH_4$ and 0.4 M NaOH, 30 °C	28,410	44.16	[68]
Co/CNA	5% $NaBH_4$ and 5% NaOH, 25 °C	2067.2	31.59	This work

temperatures. Here, $C_{NaBH4.0}$ represents the initial concentration and C_{NaBH4} represents the final concentration of its solution during the hydrolysis reaction. With the relevant dynamic calculation, if the relationship between the value of $C_{NaBH4,0}$-C_{NaBH4} and the reaction time is linear, then the $NaBH_4$ hydrolysis obeys the zero-order reaction [69,70]. In particular, the linear fit of the data shows that the correlation coefficients are above 0.995. As a result, it has been determined that the reaction kinetics in the hydrolysis of $NaBH_4$ is compatible with the zero-order.

Reusability

The reusability performance of Co/CuO–NiO–Al_2O_3 was examined to evaluate its stability in the hydrolysis of $NaBH_4$. For reusability of the Co/CuO–NiO–Al_2O_3 catalyst at 25 °C, 5 wt% $NaBH_4$, 5 wt% NaOH, and 50 mg of supported catalyst were used. After the reaction, the catalyst was filtered, washed 2–3 times with distilled water, then dried at 80 °C for 4 h. Fig. 11a shows the hydrogen production volumes obtained with Co/CuO–NiO–Al_2O_3 catalysts for five cycles. As can be seen from Fig. 11a, at the end of five cycles for Co/CuO–NiO–Al_2O_3 catalyst was obtained about 100% conversion, which also confirms the stability of the catalyst in all five

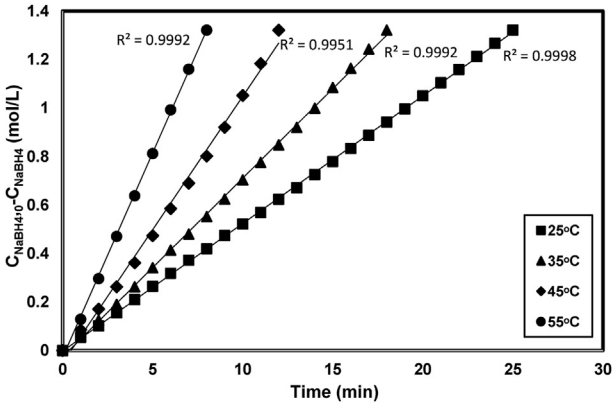

Fig. 10 – Data analyses based on zero-order reaction kinetics.

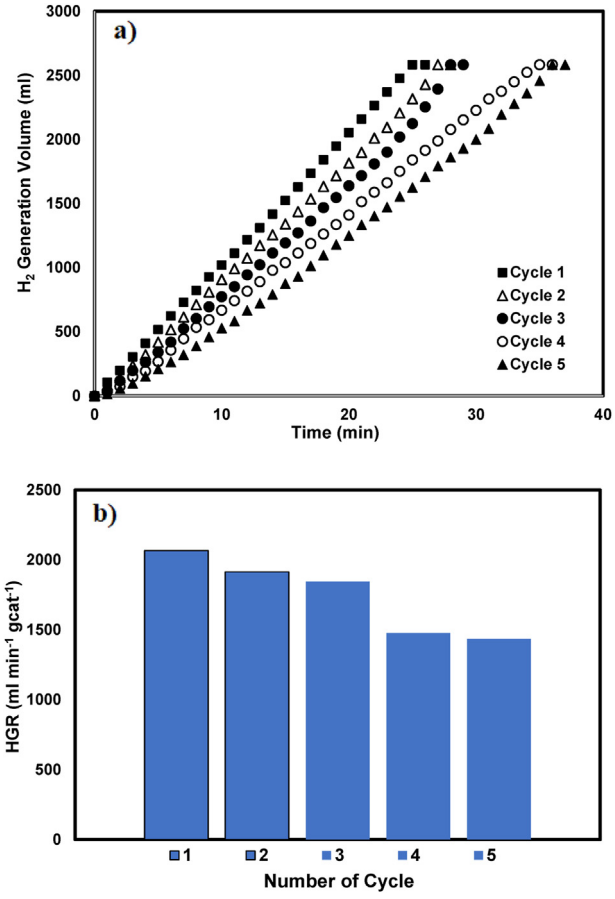

Fig. 11 – (a) Recyclability of Co/CuO–NiO–Al_2O_3 catalyst, (b) HGR values over 5 cycles.

cycles. The preservation rate of the Co/CuO–NiO–Al_2O_3 catalyst after five cycles remains at 69% of its initial catalytic activity (Fig. 11b). However, a minimum HGR even after five cycles was found as 1435.6 ml min^{-1} g_{cat}^{-1}, which was still higher than those of some other cobalt-based catalysts (Table 1). The decrease in catalytic activity is a result of the increased accumulation of sodium metaborate remaining on the catalyst surface in each reaction cycle. This causes inactivation of the catalyst surface and reduced accessibility of the active sites [71]. This is also consistent with the XRD results (Fig. 2). The obtained activity results show that the Co/CuO–NiO–Al_2O_3 catalyst is a promising candidate for the hydrolysis of $NaBH_4$.

Hydrolysis mechanism

As seen in Fig. 6, Co/Al_2O_3 catalyst shows the lowest activity. It is seen that Al_2O_3 in the support material has no effect on the catalytic activity and only increases the porosity. However, it is observed that the catalytic activity increases during the hydrolysis reaction when the support material is CuO, NiO, CuO–Al_2O_3, and NiO–Al_2O_3. Since the amount of Co-doped on these supports does not change, it is evidence that the increase in catalytic activity is due to the formation of new active sites on the CuO and NiO surfaces in the support material. We can say that these new active CuO and NiO sites formed next to the Co active sites help the generation of more hydrogen in the hydrolysis of $NaBH_4$. Co/CuO–NiO–Al_2O_3 catalyst was synthesized as trimetallic oxide support in order to compare with single and bimetallic supports and to see the combined effect of CuO and NiO sites. The highest HGR value was obtained for Co/CuO–NiO–Al_2O_3 catalyst (Fig. 6). In obtaining this high HGR value, the contribution of CuO and NiO sites, as well as Co sites, is too high to be neglected.

The several mechanisms hydrolysis of $NaBH_4$ over the metal-based catalyst in the literature have been reported [66,72–74]. Most of the reported mechanisms are based on Langmuir–Hinshelwood model. Similar to the Langmuir-Hinshelwood model we proposed a mechanism for $NaBH_4$ hydrolysis over Co/CuO–NiO–Al_2O_3 catalyst which is represented in Fig. 12. Co/CuO–NiO–Al_2O_3 catalyst involves four different active sites; Co, CuO, NiO, and O. In this mechanism, we predict that $NaBH_4$ is adsorbed on one of the active sites such as Co, CuO, and NiO and H_2O is adsorbed on one of the active sites such as CuO, NiO, and O. The hydrogen in the form of hydride (H^-) gets transferred from BH_4^- which then reacts with the water molecule to produce H_2 and OH^-. The OH^- ion produced interacts with the BH_4^- and forms the $BH_3(OH)^-$ion. At the end of three successive steps following the same procedure, all the hydrogen in the $BH_3(OH)^-$ ion is replaced by OH^- ions to form $B(OH)_4$ ion, and 4 hydrogen molecules are released.

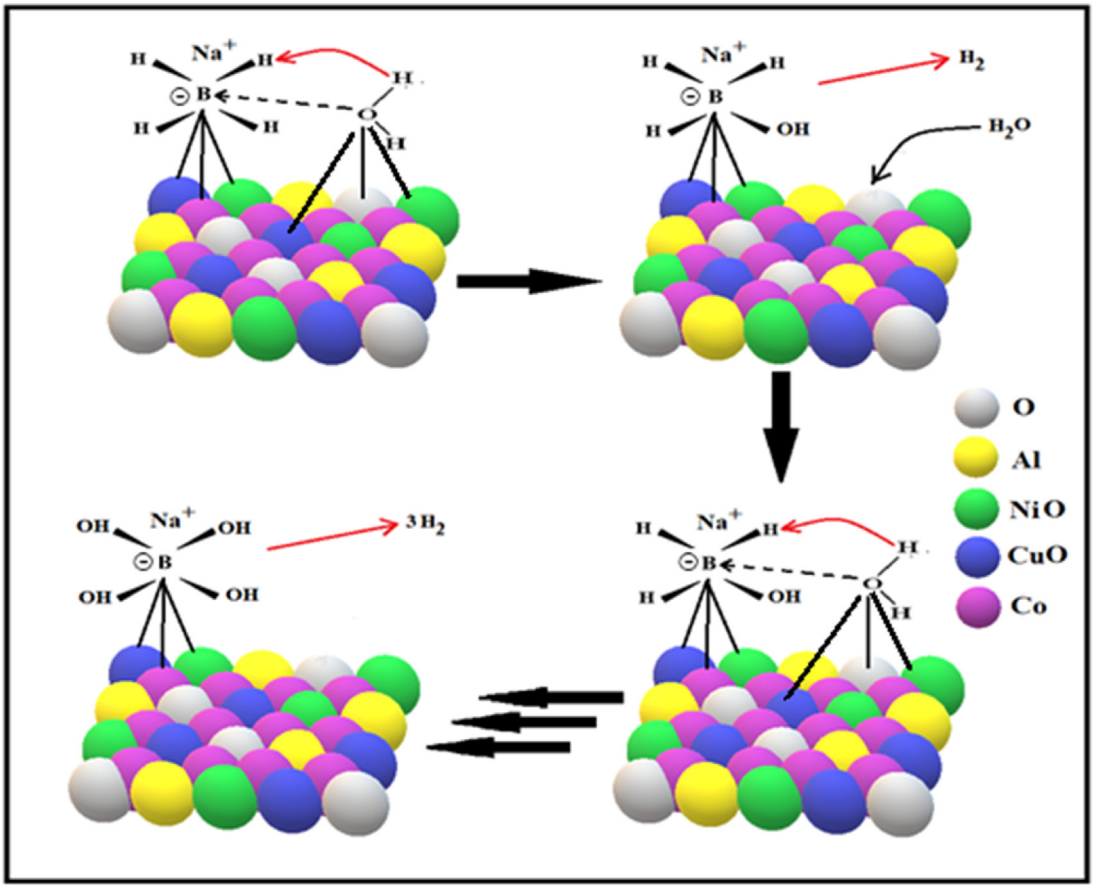

Fig. 12 – Proposed mechanism of $NaBH_4$ hydrolysis using Co/CuO–NiO–Al_2O_3 catalyst.

Conclusions

A simple and cost-effective impregnated method has been adopted to synthesize the Co-based catalysts on different support materials (Co/CuO, Co/NiO, Co/Al_2O_3, Co/NiO–Al_2O_3, Co/CuO–Al_2O_3 and Co/CuO–NiO–Al_2O_3) and their catalytic activity for hydrolysis of $NaBH_4$ have been evaluated. The effects of a solution temperature range of 25–55 °C, Co amount, and reusability have been investigated by using Co/CuO–NiO–Al_2O_3 catalyst, which is the most effective catalyst among them. The highest HGR of 6460.0 ml min^{-1} g_{cat}^{-1} has been observed at 55 °C for Co/CuO–NiO–Al_2O_3 catalyst. The activation energy determined based on zero-order reaction kinetics is 31.59 kJ mol^{-1}. Reusability experiments showed some decrease in the stability of the Co/CuO–NiO–Al_2O_3 catalyst after the first cycle. However, the Co/CuO–NiO–Al_2O_3 catalyst has been able to maintain its efficiency by 69% after the 5th cycle. There are no studies found in the literature regarding Co-based catalysts on a triplex metal oxide support. Therefore, the Co/CuO–NiO–Al_2O_3 catalyst can be used as a novel commercial catalyst for economic and large-scale production for hydrogen generation via $NaBH_4$ hydrolysis.

Declaration of competing interest

The authors declare that they have no known competing financial interests or personal relationships that could have appeared to influence the work reported in this paper.

Acknowledgments

The authors are gratefully acknowledged for financial support by Atatürk University BAP project through grant number 2021/9721.

REFERENCES

[1] Li R, Zhang F, Zhang J, Dong H. Catalytic hydrolysis of $NaBH_4$ over titanate nanotube supported Co for hydrogen production. Int J Hydrogen Energy 2022;47:5260–8.
[2] Yang L, Fan C, Zhang J, Zhang F, Li R, Yi S, et al. Poly (acrylic acid)-modified silica nanoparticles as a nonmetal catalyst for $NaBH_4$ methanolysis. Int J Hydrogen Energy 2021;46:23236–44.
[3] Dawood F, Anda M, Shafiullah GM. Hydrogen production for energy: an overview. Int J Hydrogen Energy 2020;45:3847–69.
[4] Kytsya A, Berezovets V, Verbovytskyy Y, Bazylyak L, Kordan V, Zavaliy I, et al. Bimetallic Ni-Co nanoparticles as an efficient catalyst of hydrogen generation via hydrolysis of $NaBH_4$. J Alloys Compd 2022;908:164484.
[5] Ren Y, Li Z, Deng B, Ye C, Zhang L, Wang Y, et al. Superior hydrogen evolution electrocatalysis enabled by CoP nanowire array on graphite felt. Int J Hydrogen Energy 2022;47:3580–6.
[6] Qiu Y, Feng Z, Ji X, Liu J. Surface self-reconstruction of nickel foam triggered by hydrothermal corrosion for boosted water oxidation. Int J Hydrogen Energy 2021;46:1501–8.
[7] Fang W, Liu D, Lu Q, Sun X, Asiri AM. Nickel promoted cobalt disulfide nanowire array supported on carbon cloth: an efficient and stable bifunctional electrocatalyst for full water splitting. Electrochem Commun 2016;63:60–4.
[8] Du H, Liu Q, Cheng N, Asiri AM, Sun X, Li CM. Template-assisted synthesis of CoP nanotubes to efficiently catalyze hydrogen-evolving reaction. J Mater Chem 2014;2:14812–6.
[9] Xu S, Zhao H, Li T, Liang J, Lu S, Chen G, et al. Iron-based phosphides as electrocatalysts for the hydrogen evolution reaction: recent advances and future prospects. J Mater Chem 2020;8:19729–45.
[10] Li X, Zhang R, Luo Y, Liu Q, Lu S, Chen G, et al. A cobalt–phosphorus nanoparticle decorated N-doped carbon nanosheet array for efficient and durable hydrogen evolution at alkaline pH. Sustain Energy Fuels 2020;4:3884–7.
[11] Ceyhan AA, Edebali S, Fangaj E. A study on hydrogen generation from $NaBH_4$ solution using Co-loaded resin catalysts. Int J Hydrogen Energy 2020;45:34761–72.
[12] Hayagreevan C, Siva B, Rahu R, Denisdo S, Jeevagan J, Adinaveen T, et al. Sulphonated silica and sulphonated silica/carbon particles as efficient catalysts for hydrogen generation from sodium borohydride hydrolysis. Int J Hydrogen Energy 2021;46:33849–63.
[13] Yao Q, He M, Hong X, Chen X, Feng G, Lu ZH. Hydrogen production via selective dehydrogenation of hydrazine borane and hydrous hydrazine over MoOx-promoted Rh catalyst. Int J Hydrogen Energy 2019;44:28430–40.
[14] Lu ZH, Li J, Feng G, Yao Q, Zhang F, Zhou R, et al. Synergistic catalysis of MCM-41 immobilized Cu–Ni nanoparticles in hydrolytic dehydrogeneration of ammonia borane. Int J Hydrogen Energy 2014;39:13389–95.
[15] Deng J, Sun B, Xu J, Shi Y, Xie L, Zheng J, et al. A monolithic sponge catalyst for hydrogen generation from sodium borohydride solution for portable fuel cells. Inorg Chem Front 2021;8:35–40.
[16] Santosd MF, Sequeira CAC. Sodium borohydride as a fuel for the future. Renew Sustain Energy Rev 2011;15:3980–4001.
[17] Lu YC, Chen MS, Chen YW. Hydrogen generation by sodium borohydride hydrolysis on nanosized CoB catalysts supported on TiO_2, Al_2O_3 and CeO_2. Int J Hydrogen Energy 2012;37:4254–8.
[18] Wang L, Li Z, Zhang P, Wang G, Xie G. Hydrogen generation from alkaline $NaBH_4$ solution using Co–Ni–Mo–P/γ-Al_2O_3 catalysts. Int J Hydrogen Energy 2016;41:1468–76.
[19] Shen X, Wang Q, Guo S, Liu B, Sun Z, Zhang Z, et al. Modified CoB supported on Ag-activated TiO_2 for hydrogen generation from alkaline $NaBH_4$ solution. Int J Hydrogen Energy 2015;40:6346–57.
[20] Huang W, Xu F, Liu X. Superior hydrogen generation from sodium borohydride hydrolysis catalyzed by the bimetallic Co–Ru/C nanocomposite. Int J Hydrogen Energy 2021;46:25376–84.
[21] Ma C, Duan J, Fu Y, Chang J. Hydrogen production from additive-free formic acid over highly active metal organic frameworks-supported palladium-based catalysts. Int J Hydrogen Energy 2021;46:5259–69.
[22] Han Z, Zhang RL, Duan JJ, Wang AJ, Zhang QL, Huang H, Feng JJ. Platinum-rhodium alloyed dendritic nanoassemblies: an all-pH efficient and stable electrocatalyst for hydrogen evolution reaction. Int J Hydrogen Energy 2020;45:6110–9.
[23] Bozkurt G, Özer A, Yurtcan AB. Development of effective catalysts for hydrogen generation from sodium borohydride: Ru, Pt, Pd nanoparticles supported on Co_3O_4. Energy 2019;180:702–13.
[24] Larichev YV, Netskina OV, Komova OV, Simagina VI. Comparative XPS study of Rh/Al_2O_3 and Rh/TiO_2 as catalysts for NaBH4 hydrolysis. Int J Hydrogen Energy 2010;35:6501–7.

[25] Abdelhamid HN. A review on hydrogen generation from the hydrolysis of sodium borohydride. Int J Hydrogen Energy 2021;46:726–65.
[26] Demirci UB, Miele P. Cobalt-based catalysts for the hydrolysis of $NaBH_4$ and NH_3BH_3. Phys Chem Chem Phys 2014;16:6872.
[27] Demirci UB, Akdim O, Hannauer J, Chamoun R, Miele P. Cobalt, a reactive metal in releasing hydrogen from sodium borohydride by hydrolysis: a short review and a research perspective. Sci China Chem 2010;53:1870–9.
[28] Yao Q, Ding Y, Lu ZH. Noble-metal-free nanocatalysts for hydrogen generation from boron-and nitrogen-based hydrides. Inorg Chem Front 2020;7:3837–74.
[29] Akdim O, Demirci UB, Muller D, Miele P. Cobalt (II) salts, performing materials for generating hydrogen from sodium borohydride. Int J Hydrogen Energy 2009;34:2631–7.
[30] Jeong SU, Cho EA, Nam SW, Oh IH, Jung UH, Kim SH. Effect of preparation method on Co-B catalytic activity for hydrogen generation from alkali $NaBH_4$ solution. Int J Hydrogen Energy 2007;32:1749–54.
[31] Baydaroglu F, Özdemir E, Hasimoglu A. An effective synthesis route for improving the catalytic activity of carbon-supported Co-B catalyst for hydrogen generation through hydrolysis of $NaBH_4$. Int J Hydrogen Energy 2014;39:1516–22.
[32] Ge S, Liu X, Liu J, Liu H, Liu H, Chen X, et al. Synthesis of TixSn1-xO2 mixed metal oxide for copper catalysts as high-efficiency NH3 selective catalytic oxidation. Fuel 2022;314:123061.
[33] Li Y, Zhang Y, Qian K, Huang W. Metal–support interactions in metal/oxide catalysts and oxide–metal interactions in oxide/metal inverse catalysts. ACS Catal 2022;12:1268–87.
[34] Wang Y, Qi K, Wu S, Cao Z, Zhang K, Lu Y, et al. Preparation, characterization and catalytic sodium borohydride hydrolysis of nano structured cobalt-phosphorous catalys. J Power Sources 2015;284:130–7.
[35] Wang Lina, et al. Hydrogen generation from alkaline NaBH4 solution using electroless-deposited Co–W–P supported on γ-Al_2O_3. Int J Hydrogen Energy 2015;40:7965–73.
[36] Baytar O, Izgi MS, Horoz S, Sahin O, Nar S. Al_2O_3 supported Co-Cu-B (Co-Cu-B/Al_2O_3) catalyst for hydrogen generation by hydrolysis of aqueous sodium borohydride ($NaBH_4$) solutions. Dig J Nanomater Biostruct 2019;14:673–81.
[37] Yang CC, Chen MS, Chen YW. Hydrogen generation by hydrolysis of sodium borohydride on CoB/SiO_2 catalyst. Int J Hydrogen Energy 2011;36:1418–23.
[38] Shabunya SI, Minkina VG, Kalinin VI, Sankir ND, Altaf CT. Kinetics of the catalytic hydrolysis of concentrated aqueous solutions of $NaBH_4$ on Co/TiO_2 powder. Kinet Catal 2021;62:350–9.
[39] Chang J, Tian H, Du F. Investigation into hydrolysis and alcoholysis of sodium borohydride in ethanol-water solutions in the presence of supported Co-Ce-B catalyst. Int J Hydrogen Energy 2014;39:13087–97.
[40] Tang M, Xia F, Gao C, Qiu H. Preparation of magnetically recyclable $CuFe_2O_4$/RGO for catalytic hydrolysis of sodium borohydride. Int J Hydrogen Energy 2016;41:13058–68.
[41] Liu CH, Chen BH, Hsueh CL, Ku JR, Jeng MS, Tsau F. Hydrogen generation from hydrolysis of sodium borohydride using Ni-Ru nanocomposite as catalysts. Int J Hydrogen Energy 2009;34:2153–63.
[42] Wang Y, Zou K, Zhang D, Cao Z, Zhang K, Xie Y, et al. Cobalt-copper-boron nanoparticles as catalysts for the efficient hydrolysis of alkaline sodium borohydride solution. Int J Hydrogen Energy 2020;45:9845–53.
[43] Manna J, Roy B, Pareek D, Sharma P. Hydrogen generation from $NaBH_4$ hydrolysis using Co-B/$AlPO_4$ and Co-B/bentonite catalysts. Catal Struct React 2017;3:157–64.
[44] Saka C, Salih Eygi M, Balbay A. CoB doped acid modified zeolite catalyst for enhanced hydrogen release from sodium borohydride hydrolysis. Int J Hydrogen Energy 2020;45:15086–99.
[45] Bozkurt G, Özer A, Yurtcan AB. Hydrogen generation from sodium borohydride with Ni and Co based catalysts supported on Co_3O_4. Int J Hydrogen Energy 2018;43:22205–14.
[46] Kaur Arshdeep, Gangacharyulu D, Bajpai Pramod K. Catalytic hydrogen generation from $NaBH_4/H_2O$ system: effects of catalyst and promoters. Braz J Chem Eng 2018;35:131–40.
[47] Ai LH, Gao XY, Jiang J. In situ synthesis of cobalt stabilized on macroscopic biopolymer hydrogel as economical and recyclable catalyst for hydrogen generation from sodium borohydride hydrolysis. J Power Sources 2014;257:213–20.
[48] Wang F, Zhang Y, Wang Y, Luo Y, Chen Y, Zhu H. Co-P nanoparticles supported on dandelion-like CNTs-Ni foam composite carrier as a novel catalyst for hydrogen generation from $NaBH_4$ methanolysis. Int J Hydrogen Energy 2018;43:8805–14.
[49] Zhou E, Tian L, Cheng Z, Fu C. Design of NiO flakes@$CoMoO_4$ nanosheets core-shell architecture on Ni foam for high-performance supercapacitors. Nanoscale Res Lett 2019;14:1–11.
[50] Khan MA, Nayan N, Ahmad MK, Soon CF. Surface study of CuO nanopetals by advanced nanocharacterization techniques with enhanced optical and catalytic properties. Nanomaterials 2020;10:1298.
[51] Uzundurukan A, Devrim Y. Carbon nanotube-graphene hybrid supported platinum as an effective catalyst for hydrogen generation from hydrolysis of ammonia borane. Int J Hydrogen Energy 2019;44:26773–82.
[52] Mahmood J, Jung SM, Kim SJ, Park J, Yoo JW, Baek JB. Cobalt oxide encapsulated in C_2N-h2D network polymer as a catalyst for hydrogen evolution. Chem Mater 2015;27:4860–4.
[53] Wei Y, Wang Y, Wei L, Zhao X, Zhou X, Liu H. Highly efficient and reactivated electrocatalyst of ruthenium electrodeposited on nickel foam for hydrogen evolution from $NaBH_4$ alkaline solution. Int J Hydrogen Energy 2018;43:592–600.
[54] Chen W, Xiao X, He J, Dong Z, Wang X, Chen M, et al. A dandelion-like amorphous composite catalyst with outstanding performance for sodium borohydride hydrogen generation. Int J Hydrogen Energy 2021;46:10809–18.
[55] Wei L, Ma M, Lu Y, Zhang S, Gao J, Dong X. Electrodeposited Co–Zn on Ni foam as efficient catalysts for hydrogen generation from hydrolysis of sodium borohydride. Functional Materials Letters 2017;10:1750065.
[56] Balbay A, Selvitepe N, Saka C. Fe doped-CoB catalysts with phosphoric acid-activated montmorillonite as support for efficient hydrogen production via $NaBH_4$ hydrolysis. Int J Hydrogen Energy 2021;46:425–38.
[57] Didehban A, Zabihi M, Babajani N. Preparation of the efficient nano-bimetallic cobalt-nickel catalysts supported on the various magnetic substrates for hydrogen generation from hydrolysis of sodium borohydride in alkaline solutions. Polyhedron 2020;180:114405.
[58] Kıpçak İ, Kalpazan E. Preparation of CoB catalysts supported on raw and Na-exchanged bentonite clays and their application in hydrogen generation from the hydrolysis of $NaBH_4$. Int J Hydrogen Energy 2020;45:26434–44.
[59] Liang Y, Wang P, Dai HB. Hydrogen bubbles dynamic template preparation of a porous Fe–Co–B/Ni foam catalyst for hydrogen generation from hydrolysis of alkaline sodium borohydride solution. J Alloys Compd 2010;491:359–65.
[60] Lee J, Kong KY, Jung CR, Cho E, Yoon SP, Han J, et al. A structured Co–B catalyst for hydrogen extraction from $NaBH_4$ solution. Catal Today 2007;120:305–10.

[61] Su CC, Shih YJ, Huang YH, Lu MC. Synthesis and characterization of Co/SiO_2 as catalyst catalyze hydrogen generation. Mater Lett 2011;65:3212–5.
[62] Kim DH, Jo S, Kwon J, Lee S, Eom K. Effect of iron content on the hydrogen production kinetics of electroless-deposited CoNiFeP alloy catalysts from the hydrolysis of sodium borohydride, and a study of its feasibility in a new hydrolysis using magnesium and calcium borohydrides. Int J Hydrogen Energy 2019;44:15228–38.
[63] Li Z, Wang L, Zhang Y, Xie G. Properties of CuCoP/γ-Al_2O_3 catalysts for efficient hydrogen generation by hydrolysis of alkaline $NaBH_4$ solution. Int J Hydrogen Energy 2017;42:5749–57.
[64] Shih YJ, Su CC, Huang YH, Lu MC. SiO_2-supported ferromagnetic catalysts for hydrogen generation from alkaline $NaBH_4$ (sodium borohydride) solution. Energy 2013;54:263–70.
[65] Abdelhamid HN. Dehydrogenation of sodium borohydride using cobalt embedded zeolitic imidazolate frameworks. J Solid State Chem 2021;297:122034.
[66] Kassem AA, Abdelhamid HN, Fouad DM, Ibrahim SA. Metal-organic frameworks (MOFs) and MOFs-derived CuO@C for hydrogen generation from sodium borohydride. Int J Hydrogen Energy 2019;44:31230–8.
[67] Abdelhamid HN. Solid acid zirconium oxo sulfate/carbon-derived UiO-66 for hydrogen production. Energy Fuels 2021;35:10322–6.
[68] Yao L, Li X, Peng W, Yao Q, Xia J, Lu ZH. Co-CeOx nanoparticles anchored on a nitrogen-doped carbon nanosheet: a synergistic effect for highly efficient hydrolysis of sodium borohydride. Inorg Chem Front 2021;8:1056–65.
[69] Deonikar Virendrakumar G, et al. Hydrogen generation from catalytic hydrolysis of sodium borohydride by a Cu and Mo promoted Co catalyst. J Ind Eng Chem 2020;86:167–77.
[70] Wang Jin, et al. Efficient hydrolysis of alkaline sodium borohydride catalyzed by cobalt nanoparticles supported on three–dimensional graphene oxide. Mater Res Bull 2017;95:204–10.
[71] Huang YH, Su CC, Wang SL, Lu MC. Development of Al2O3 carrier-Ru composite catalyst for hydrogen generation from alkaline NaBH4 hydrolysis. Energy 2012;46:242–7.
[72] Demirci UB, Miele P. Reaction mechanisms of the hydrolysis of sodium borohydride: a discussion focusing on cobalt-based catalysts. Compt Rendus Chem 2014;17:707–16.
[73] Patil KN, Prasad D, Manoorkar VK, Nabgan W, Nagaraja BM, Jadhav AH. Engineered nano-foam of tri-metallic (FeCuCo) oxide catalyst for enhanced hydrogen generation via $NaBH_4$ hydrolysis. Chemosphere 2021;281:130988.
[74] Bandal HA, Jadhav AR, Kim H. Cobalt impregnated magnetite-multiwalled carbon nanotube nanocomposite as magnetically separable efficient catalyst for hydrogen generation by NaBH4 hydrolysis. J Alloys Compd 2017;699:1057–67.